A Fully-Integrated Microfabricated Externally-Wetted Electrospray Thruster

IEPC-2007-233

Presented at the 30th International Electric Propulsion Conference, Florence, Italy
September 17-20, 2007

B. Gassend,* L. F. Velásquez-García,† A. I. Akinwande‡

and M. Martínez-Sánchez§

Massachusetts Institute of Technology, Cambridge, Massachusetts, 02139, USA

This paper reports the performance of a fully-integrated MEMS planar electrospray thruster array operating in the pure ion-emission regime. Electrospray thrusters work by electrostatically extracting and accelerating ions or charged droplets from a liquid surface to produce thrust. Emission occurs from sharp emitter tips, which enhance the electric field and constrain the emission location. Electrospray propulsion is desirable for its simplicity, high thrust efficiency and tunable specific impulse. However, the electrospray process limits the thrust from a single tip. Consequently, achieving millinewton thrust levels requires an array with tens of thousands of emitters.

We have used silicon batch microfabrication technology to make an array of 502 emitters in a 113 mm^2 area. The thruster, weighing 5 g, was tested with the ionic liquid EMI-BF_4, and was previously shown to operate in the pure ion-emission regime, with a total thrust of up to 13 μN and a 3000 s specific impulse. Typical operating ranges are from 500 V to 2000 V. Imprints taken by firing the emitter array against a target show all the emitters operating. Emission non-uniformities occur with a wavelength of a few emitter spacings, compatible with fabrication non-uniformities, but not with competition between neighboring emitters. Temperature-dependent current-voltage characteristics are reported which could be explained by Iribarne-Thompson ion evaporation directly from the liquid surface without formation of a Taylor cone. This emission regime had not been hypothesized heretofore.

Nomenclature

α	= Effective emission area.
β	= Field factor.
ϕ	= Free energy of ion evaporation.
A, B, C	= Parameters used when fitting the Iribarne-Thompson model.
ϵ_0, q	= Permittivity of vacuum and elementary charge.
σ	= Surface charge density.
E	= Electric field.
h, k	= Planck's constant and Boltzmann's constant.
I, j	= Emitted current and current density.
R_{model}	= Modeled resistance of leakage to extractor.
T	= Absolute temperature.
V	= Extraction voltage.

*Research Assistant, MIT Department of Electrical Engineering and Computer Science, gassend@alum.mit.edu

†Research Scientist, MIT Department of Aeronautics and Astronautics and Microsystems Technology Laboratories, lfvelasq@mit.edu

‡Professor, Department of Electrical Engineering and Computer Science, akinwand@mtl.mit.edu

§Professor, Department of Aeronautics and Astronautics mmart@mit.edu

I. Introduction

This paper presents additional performance measurements made on a previously reported microfabricated MEMS electrospray thruster.[1] This microfabricated planar electrospray thruster array with 502 emitters, and weighing 5 g, was shown to operate in the pure ion emission regime using the ionic liquid EMI-BF_4. Beam current and divergence measurements, combined with time-of-flight measurements suggested thrusts up to 13 μN with a specific impulse around 3000 s. Typical operating ranges are from 500 V to 2000 V. The present paper reports imprints obtained by firing the emitters against a smooth plate, and temperature-dependent current-voltage characteristics.

In an electrospray thruster, charged particles are electrostatically extracted from a liquid surface and accelerated. In the pure ion regime, the extracted particles are ions. Emission takes place from the tip of a Taylor cone,[2] a structure which forms when a liquid surface is placed in a sufficiently strong electric field. In order to enhance the field, the Taylor cone is usually at the tip of a sharp emitter structure. An extractor electrode with an aperture for the emitted beam produces the field. The thrust which can be obtained from a single emitter is limited by the electrospray physics to about 100 nN in the pure ion regime that is most efficient for propulsion. Arrays of emitters must be used to achieve higher thrust levels, and broaden the possible range of missions. Batch microfabrication techniques are well suited to producing these arrays cheaply, with relatively good uniformity, and at a scale where large electric fields can easily be produced.

Electrospray propulsion has numerous promising features. It reduces tankage mass by using unpressurized liquid propellant. It is highly efficient in the pure ion emission regime, requiring only 7 to 8 eV to produce an ion,[3] and having a small velocity spread in the emitted beam. With an accelerator electrode downstream of the extractor electrode, the specific impulse of the thruster can be tuned from around 500 s to many thousands of seconds, limited only by the available power and breakdown resistance of the insulators. Finally, the overall design is very simple.

A number of microfabricated electrospray thrusters have been previously reported.[4–9] The thruster reported in this paper is unique because it is a planar array operating in the pure ion emission regime with an integrated extractor electrode. In Ref. 10 we presented a thruster that made similar claims using a different extractor assembly technique. However, with that thruster, we were unable to get stable enough operation to run time-of-flight measurements and properly characterize the emitted beam.

II. The Microfabricated MEMS Thruster

The thruster is made using Deep Reactive Ion Etching (DRIE) and wafer bonding techniques, in a six mask fabrication process, and comprises two components. The emitter die in Figures 1(a) and 1(b) with 216 or 502 emitters in a 113 mm^2 area, is formed using DRIE and SF6 etching, and is plasma treated to transport liquid to the tips in a porous black-silicon surface layer.[6] In these experiments, the whole propellant supply is contained in this porous layer. The extractor die in Figure 1(c) incorporates the extractor electrode, a Pyrex layer for insulation, and springs which are used to reversibly assemble the emitter die.[11,12] This versatile assembly method, with 10 μm RMS alignment accuracy and 1.3 μm RMSD repeatability, allows the extractor die to be reused with multiple emitter dies, and potentially with different emitter concepts than the one presented. A cross-section of the thruster is shown in Figure 1(d). Full fabrication details can be found in Ref. 13.

III. Experimental Results

This section reports the results of two experiments that were not included in our previous report on this thruster:[1] imprints formed by firing the emitters against a smooth plate, and temperature-dependent current-voltage characteristics. Analysis of the measurements is deferred to Section IV, and discussion to Section V.

III.A. Thruster Preparation

The thruster was fired with the ionic liquid EMI-BF_4.[14] An estimated 0.1 to 1 mm^3 of propellant was supplied to the emitter die using a syringe and allowed to spread across the black-silicon surface. Once wetted, the emitter die was assembled to the extractor component, and the assembly was mounted on a

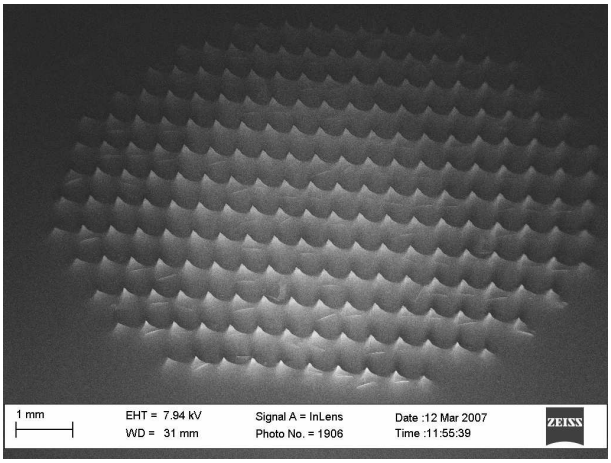

(a) 216-emitter die.

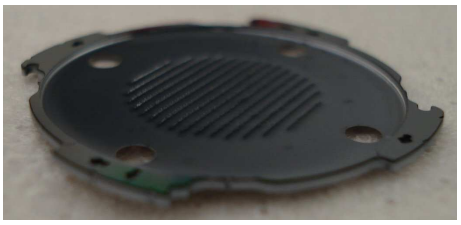

(b) 502-emitter die.

(c) Extractor die (after firing) seen from the bottom.

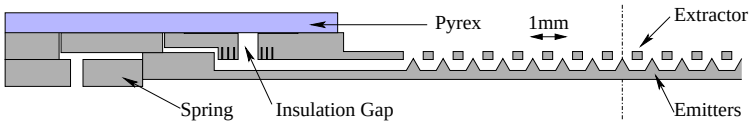

(d) Cross-section

Figure 1. The microfabricated MEMS electrospray thruster array.

high density polyethylene holder. Electrical contact to the thruster was made via copper tape and a flexible clamp which also held the thruster in place on the holder. Measurements suggest contact resistances of the order of 100 kΩ during operation. Experiments were carried out at base pressures below $1 \cdot 10^{-5}$ torr.

III.B. Emission Imprints

In this experiment, a 216-emitter die was placed in front of a conductive polished silicon plate and fired. Patterns that appeared on the plate during the experiment were observed to evaluate the uniformity of emission. The experimental setup is shown in Figure 2. Other experiments have been conducted using Indium-Tin Oxide (ITO)-coated glass, which could allow the time dependence of the emission distribution to be determined, by looking through the target as the emitters are fired.[13]

III.B.1. High Current

In this test, the thruster behaved very stably in the positive polarity, but had inconsistent behavior in the negative polarity. Voltages up to 2500 V were applied, and currents up to 70 μA were observed.

Figure 3 shows the target upon inspection. Thirteen rows are clearly visible, corresponding to the thirteen rows of emitters. In one corner of the target imprint a black/orange substance is visible. The rows cut through this substance. Microscopic examination reveals that each row is made up of erratic patterns spaced 500 μm apart, consistent with the emitter spacing. These erratic patterns have a roughly threefold symmetry, which may be due to the fact that the emitter tips have three ridge lines leading up to them.

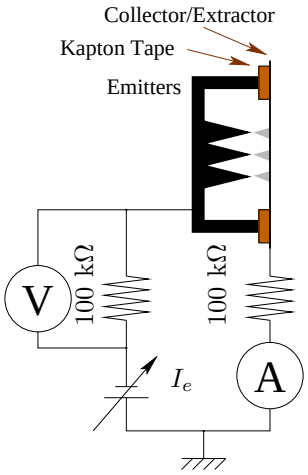

Figure 2. Firing against a plate to determine the cumulative emission imprint

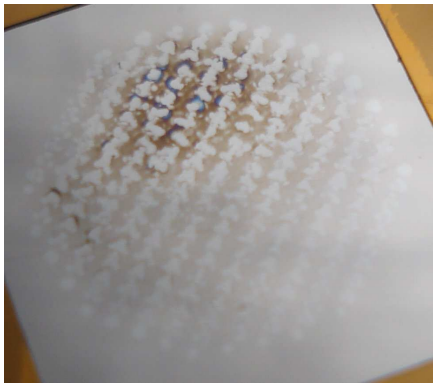

(a) All thirteen rows of emitters fired along their whole length

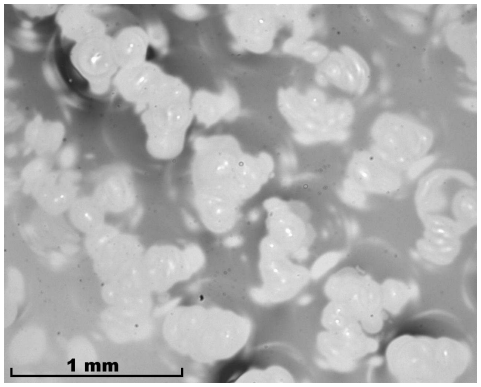

(b) Microscope image of the target, showing an array of imprints with vaguely threefold symmetry

Figure 3. Silicon target after high-current firing

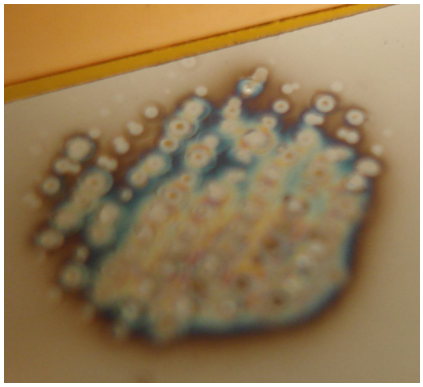

(a) Only nine rows out of thirteen are visible. (The Kapton tape has been moved since the thruster was fired.)

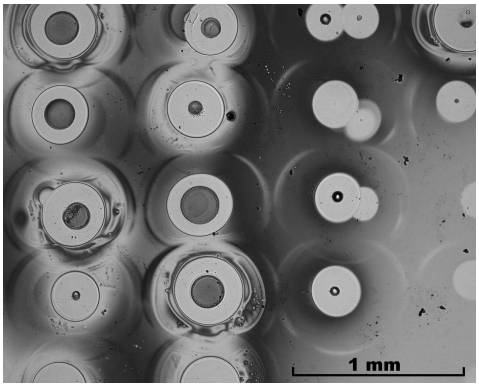

(b) Microscope image showing clean circular marks on the target

Figure 4. Silicon target after low-current firing

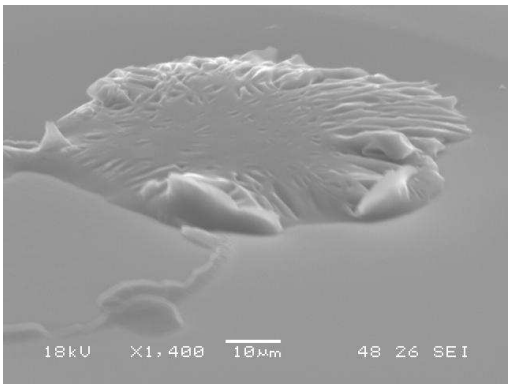

(a) The central dark spot is not flat

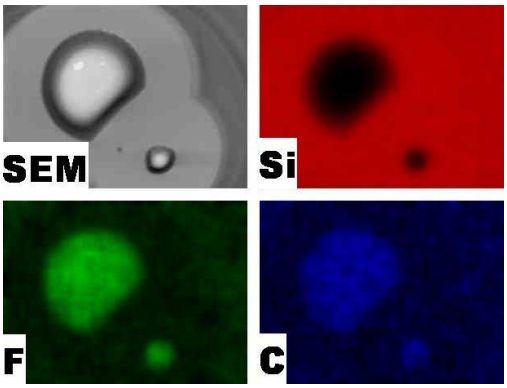

(b) EDX revealing elements present around a spot.

Figure 5. SEM and EDX observation of the low-current silicon target

Circle	Radius (μm)	Emission half-angle (°)
Inner Orange Circle (max)	200	12
Clean Circle (small)	250	15
Clean Circle (large)	350	21
Outer Halo	500	29
Pencils in Ref. 6		9.5
Volcanoes in Ref. 6		14.1

Table 1. Approximate feature sizes on the low-current silicon target

III.B.2. Low Current

To determine if the previously observed erratic patterns are due to the high current levels, the next experiment was carried out at a low current level of a few hundred nanoamps. The emitters were fired for about an hour at this current level before they were inspected.

This time only nine (of a total of thirteen) incomplete rows are visible, suggesting that not all the emitters fired (see Figure 4). The emitters that did not fire may have been less sharp than those that did fire, or the emitter die may have been slightly tilted relative to the silicon plate, causing a disparity in electric field between emitters. In any case, in the regions that did fire, all the emitters were firing, as attested to by neat rows of circles, 250 to 350 μm in diameter (see Figure 4). Many of the circles contain darker dots up to 200 μm in diameter, and each circle is surrounded by a roughly circular halo 500 μm in diameter.

In this experiment, a single 300 μm layer of tape was used, and the emitters were an estimated 150 μm below the top surface of the emitter die, so the total emitter to plate distance was 450 μm. Table 1 summarizes the emission half-angles that would produce the different circles that were observed (i.e., the half angle of the cone with its tip at the emitter tip and which passes through the circle).

Scanning Electron Microscopy (SEM) and Energy Dispersive X-Ray (EDX) spectroscopy[15] shown in Figure 5 revealed more details on the circular patterns that were observed. The central spot appears to have some topography on the micron scale, while the area outside the clean circle does not have this topography (not shown). EDX spectroscopy reveals Carbon and Fluorine in the central spot, but no silicon, implying that the spot has at least micron-scale thickness. Around the spot is an area with pure silicon, and further out a weak fluorine and carbon signal reappears. There was no visible etching of the silicon target.

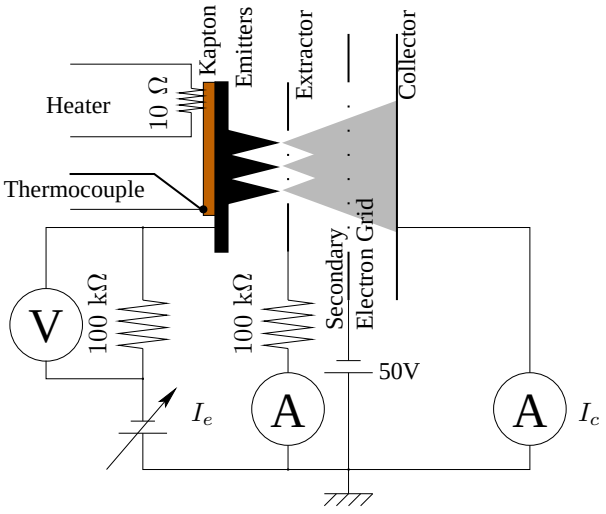

Figure 6. Experimental setup to take the temperature dependent I-V characteristic of the thruster.

III.C. Temperature Dependence

In this experiment, the temperature dependence of emission was measured by heating one side of the thruster with a 10 Ω resistor, and monitoring the temperature on the other side of the thruster using a thermocouple. The experiment was conducted without a proper feedthrough for the thermocouple, so some inaccuracy in the temperature reading is expected. Experiments were run between 30 and 70°C. Starting with the thruster at room temperature, the thruster was turned on and 15 second IV sweeps were made. This method gives good temperature resolution, but poor voltage resolution. Since the measurements were made as the temperature was rising,

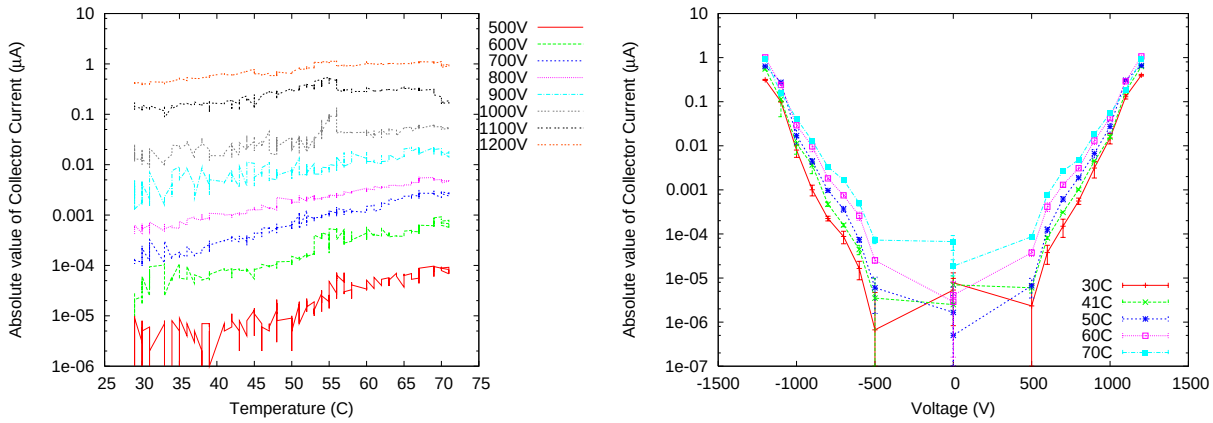

(a) Temperature dependence

(b) IV characteristics

Figure 7. Current dependence on temperature for the dynamic experiment

there was a lag between the temperature indicated by the thermocouple and the temperature of the emitters. Measurements taken when the heater was turned off and the thruster was cooling suggest an offset of up to 5°C between the measured temperature and the emitter temperature.

The Current-Voltage (I-V) characteristic of the 502-emitter array was measured with the experimental setup shown in Figure 6. The array was fired against a grounded collector plate. Currents to the collector and extractor were measured using Keithley 6514 and 6517A electrometers. A secondary electron suppression grid was placed in front of the collector plate, and biased to -50 V.

Figure 7 shows the dependence of the emitted current on temperature. The only contribution to this current is particles emitted from the thruster and collected on the collector plate. Figure 8 shows the dependence of the extractor current on temperature, a combined measure of emitted particles intercepted by the extractor and of leakage through the insulator.

IV. Analysis

This section presents some analysis of the temperature dependent current data in an attempt to explain it. First the leakage current is considered, and then the collected current is modeled as a fixed-geometry ion evaporation process.

IV.A. Leakage Current

The temperature dependence of the extractor current in Figure 8(a) shows two exponential trends which have been plotted. Assuming Arrhenius processes, the activation temperature is 10000°K (0.86 eV) at low temperature and 21500°K (1.85 eV) at high temperature.

Plotting resistance instead of current as in Figure 8(b) yields additional insight, as the high temperature plots all coincide, showing an ohmic behavior (resistance independent of voltage). The high temperature behavior is consistent with ionic conduction in the Pyrex insulator causing leakage between the emitters and the extractor.[a] The origin of the low temperature extractor current is currently undetermined.

IV.B. Ion Evaporation

Electrospray is a complex process involving the solution of a multi-scale electrostatic free boundary problem, coupled with fluid flow, and charge relaxation. Observations made on electrospray from capillary tubes show that, as the electric field is increased, the liquid meniscus at the tip of the capillary deforms until it suddenly

[a]A subsequent experiment without the liquid or the emitters revealed the same drop in resistance with temperature, strengthening the case for leakage through the Pyrex. Unfortunately, a thermocouple failure prevented this experiment from revealing whether the presence of wetted emitters affects the low-temperature resistance.

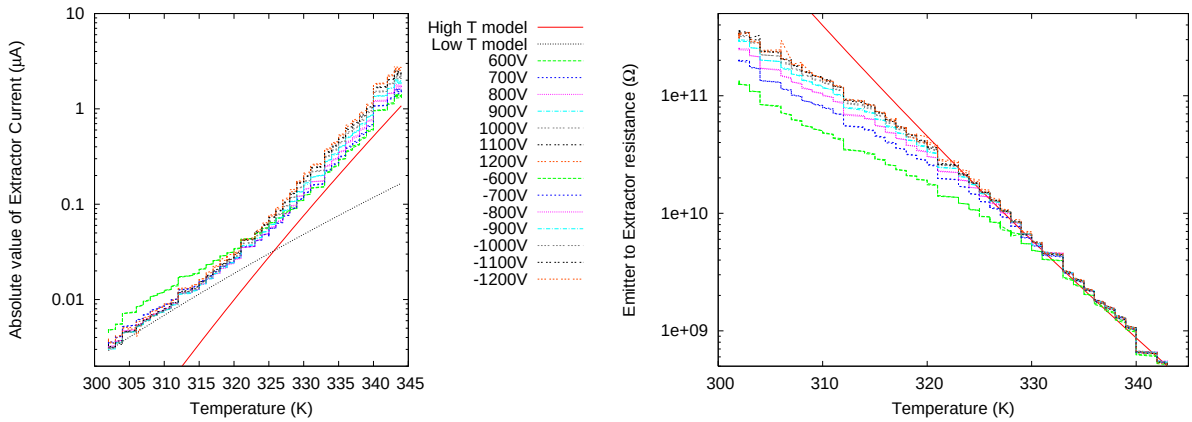

(a) (b)

Figure 8. Leakage to the extractor, due to beam interception and leakage through the insulator, as a function of temperature. The resistance (i.e., voltage to current ratio) is also plotted. Exponential temperature dependence with Arrhenius activation temperatures of 10000°K (0.86 eV) at low temperature and 21500°K (1.85 eV) at high temperature are apparent. The high temperature resistance is well approximated by $R_{\text{model}}(T) = 3 \cdot 10^{-19}\, e^{-\frac{21500}{T}}$

transitions into a Taylor cone shape. This transition coincides with the onset of current emission from the emitter. For emitters with a porous surface layer, it had been assumed that the same process takes place, albeit at a smaller scale (which prevents direct observation of the Taylor cone formation). Indeed, previous observations[6] show an abrupt onset of current emission.

For the thruster presented here, we were unable to observe the onset of emission. The measured current climbs out of the noise floor (below 100 pA) and steadily climbs from there. This behavior could be explained by a starting current below the noise floor, but this sections considers a different hypothesis in which emission takes place without a significant deformation of the liquid surface or formation of a Taylor cone.

Indeed, consider a conductive liquid surface subjected to a strong electric field. For a large enough field, ions can be directly extracted from the liquid surface by the process of Iribarne-Thompson ion evaporation,[16] for which a concise derivation can be found in Ref. 17. In this model, the ion evaporation current density is given by

$$j = \frac{\sigma k T}{h} e^{-\frac{q\phi - \sqrt{q^3 E/(4\pi\epsilon_0)}}{kT}}, \tag{1}$$

where k is Boltzmann's constant, T is the absolute temperature, h is Planck's constant, ϕ is the free energy of ion evaporation (in eV), E is the electric field, q is the charge of the emitted ions, σ is the surface charge, and ϵ_0 is the permittivity of vacuum. Setting $\sigma = \epsilon_0 E$, and introducing a field factor β and an effective emission area α, such that $E = \beta V$ and $I = \alpha J$, we get a formula for the emitted current as a function of applied voltage

$$I = \frac{\alpha \epsilon_0 \beta V k T}{h} e^{-\frac{q\phi - \sqrt{q^3 \beta V/(4\pi\epsilon_0)}}{kT}}. \tag{2}$$

Rearranging, we get

$$T \ln\left(\frac{I}{VT}\right) = T \ln\left(\frac{\alpha \epsilon_0 \beta k}{h}\right) - \frac{q\phi}{k} + \sqrt{\frac{q^3 \beta}{4\pi\epsilon_0 k^2}}\sqrt{V} = AT - B + C\sqrt{V}. \tag{3}$$

Therefore, for a liquid surface with constant geometry, $T \ln\left(\frac{I}{VT}\right)$ as a function of T and $\sqrt{V}$ defines a plane. The slope in the T direction is A, the slope in the $\sqrt{V}$ direction is C, and the intercept is $-B$. Thus, plotting slices of this plane in the T and $\sqrt{V}$ directions yields the values of A, B and C, from which the free energy of ion evaporation ϕ, the field factor β and the effective area α can be deduced using

$$\phi = \frac{BkT}{q} \tag{4}$$

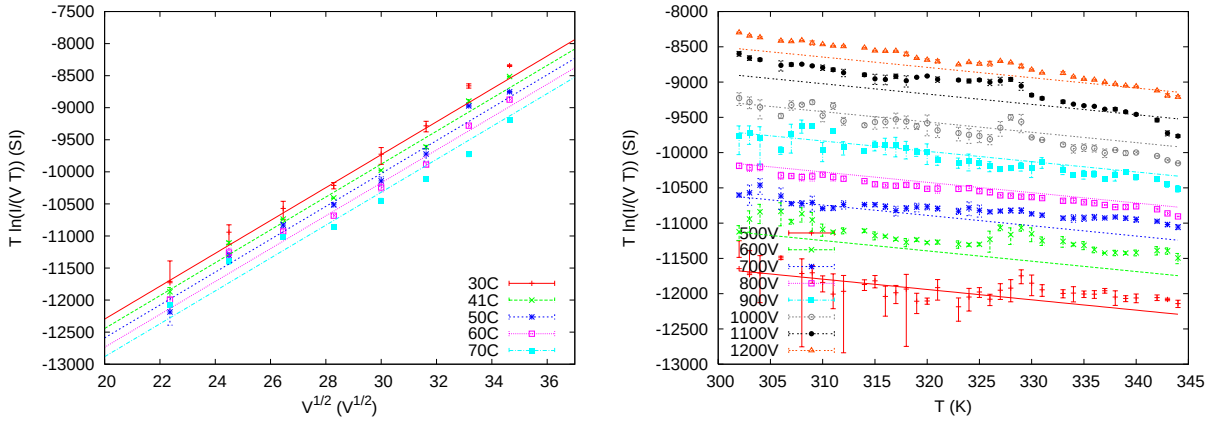

(a) Plot of $T \ln\left(\frac{I}{VT}\right)$ as a function of $\sqrt{V}$. The slope is C and the intercept is $AT - B$

(b) Plot of $T \ln\left(\frac{I}{VT}\right)$ as a function of T. The slope is A and the intercept is $-B + C\sqrt{V}$

Figure 9. Modeling ion emission using the Iribarne-Thompson model, taking $\phi = 1.12$ V, $\beta = 3.4 \cdot 10^3$ cm^{-1} and $\alpha = 6.9 \cdot 10^{-12}$ m^2. Only low current data is available here (up to 1 nA/emitter)

$$\beta = \frac{4\pi\epsilon_0 k^2 C^2}{q^3} \tag{5}$$

$$\alpha = \frac{e^A h}{\epsilon_0 \beta k} \tag{6}$$

Directly applying this method to electrospray seems difficult because the geometry of the liquid surface is unknown a priori. Emission could be taking place from the tip of a Taylor cone with a tip radius that is unknown to us. Moreover, protrusions could emanate from the tip of the cone, further enhancing the field in a difficult to predict manner. It is therefore unexpected to see parallel straight lines appear in figures 9, in which the data from Figure 7(b) have been replotted. Using Equation (3), we find $\phi = 1.12$ V, $\beta = 3.4 \cdot 10^3$ cm^{-1} and $\alpha = 6.9 \cdot 10^{-12}$ m^2 (or $1/\beta = 2.9$ μm and $\sqrt{\alpha/\pi}$ =1.5 μm). For a 500 V applied voltage, the field at the emission site is 0.15 V/nm. The standard deviation of $\log_{10}(I_{\text{meas}}/I_{\text{calc}})$ is 0.23, which corresponds to an error factor of 1.8.

The fitted parameters have reasonable orders of magnitude, so the temperature dependent data is consistent with emission from a liquid surface that does not significantly deform with voltage. We defer further discussion on this possibility to the following section.

V. Discussion

In the imprints that were made (Figures 3 and 4), neighboring emitters produce similar looking spots, suggesting comparable time-averaged emission. Thus negative feedback of one emitter on its neighbors through the propellant supply or the electric field does not seem sufficient to cause an instability in which the first emitter that fires prevents its neighbors from firing, or if such an instability does occurs, it is not steady and the emitter that is firing is constantly shifting. However, there are non-uniformities across the array of emitters which could be due to: non-uniform wetting of the emitter die, non-uniform height and emitter sharpness due to the fabrication process (with slow radial variations across the wafer and variations between the center and the periphery of individual emitter arrays), and tilt between the emitter die and the target.

The circular spots observed on the target at low current levels (Figure 3(b)) suggest a highly symmetric beam emanating from the emitter tip. The pattern of concentric rings deserves some explanation. Figure 10 depicts one hypothetical mechanism to form this pattern. This mechanism relies on the existence of an over-wet phase,[1] during which a freshly refuelled thruster emits erratically before settling into the stable operation that has been the focus of the present paper. In the over-wet phase, droplets are emitted and form a deposit on the target with maximum thickness directly in front of the emitter. Then in steady phase, pure

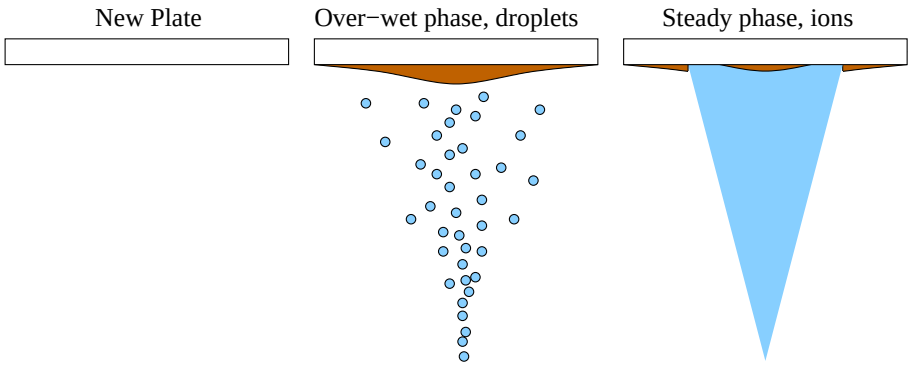

Figure 10. A hypothetical set of events which could produce the observed circular patterns on the target. Starting from a clean plate, first a thick layer is deposited in the droplet regime. Then ion emission occurs, clearing off part of the deposited material. A region of deposit remains in the center of the cleaned out area where the deposit was thickest, or where the ion flux was lower

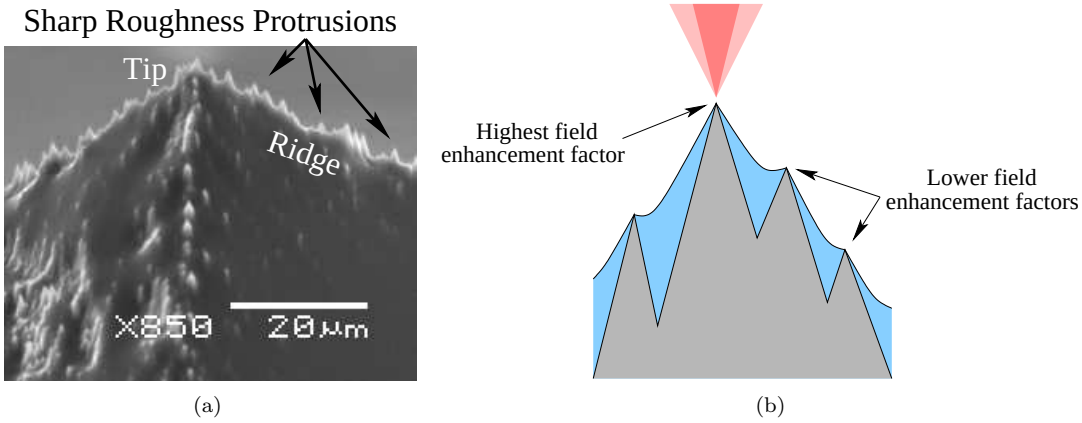

Figure 11. Closeup of a wetted pyramidal emitter tip showing sharp surface roughness features, particularly along the ridge lines (a). These sharp features may create sufficient field enhancement for ion emission without Taylor cone formation (b).

ion emission occurs. The ions sputter away the deposited material over a circular region, getting through the thinner parts before the thicker parts, which results in the observed clean-dirty-clean concentric pattern.

At higher current levels, the erratic pattern that is observed (Figure 4(b)) suggests emission from multiple locations per emitter. The emitters that were used are shaped like a triangular pyramid near the tip, and the threefold symmetry of the target pattern could be related to the ridges of the pyramid. Indeed, the surface roughness creates many sharp protrusions along the ridges of the pyramid as seen in Figure 11(a), which could serve as emission sources at high field strengths.

The analysis in Section IV.B showed that the temperature-dependent current data is consistent with ion-evaporation limited emission from a liquid surface with fixed field factor β, and hence with fixed geometry. The simplest explanation for this compatibility is that emission is taking place without the formation of a Taylor cone. Thus the liquid surface has roughly the same geometry whether or not the electrospray is operating. The fact that the surface roughness on the emitters is formed from many sharp tips may contribute to the operation without a Taylor cone, since it can pin the liquid surface in a conical configuration, even without an applied voltage (see Figure 11(b)).

Because of the strong dependence of I on β it is likely that there is significant non-uniformity in emission between emitters, as a small change in emitter geometry will cause a large variation in current. This situation could change at higher currents than are covered by the temperature-dependent data reported here. Indeed, at higher currents, we expect that hydraulic impedance will begin to have an effect by limiting the availability

of liquid at the emission site. This could have a ballasting effect, causing emission to be more uniformly distributed between the emitters. At sufficiently high applied voltages, emission sites farther from the tip will achieve sufficient fields to begin emitting. Sharp features along the emitter ridges should have the highest field factor, which could lead to the irregular emission patterns with threefold symmetry in Figure 3(b).

If the hypothesis of emission without Taylor cone formation is confirmed, it would be analogous to a behavior observed with liquid metal ion sources, for which a small amount of emission sometimes precedes the formation of a Taylor cone.[18] In our case, the presence of sharp surface roughness features (as seen in Figure 11(a)) may allow a conical liquid surface supported by the surface roughness to form, allowing high field enhancement and ion emission before the surface is destabilized into a Taylor cone.

From the temperature dependent current experiments, it appears that temperature control of the thruster, while possible, only provides a small tuning range, insignificant compared with the orders-of-magnitude tuning obtained by varying the applied voltage. Combined with the fact that temperature significantly increases extractor current, probably via leakage through the Pyrex insulation, temperature does not seem like a useful control parameter. Temperature control may nevertheless be useful to independently set thrust and specific impulse. However, the addition of an accelerator electrode would have the same effect in a simpler and more versatile manner.

VI. Conclusion

Additional characterization of our fully integrated MEMS planar electrospray thruster has been presented. Imprints created by firing emitters against a target plate show good uniformity at high spatial frequencies but some non-uniformities across an array. Low current imprints are suggestive of circular emitted beams that degrade into erratically shaped beams at higher current levels. Temperature dependent current-voltage characteristics show a moderate increase in emitted current with temperature, but a high increase in the current measured on the extractor electrode, probably due to leakage in the Pyrex insulator. Thus, temperature control of thrust does not appear useful, especially given the ease with which voltage can control thrust. The temperature dependent current-voltage characteristics are compatible with ion evaporation from a constant-geometry meniscus, which suggests the possibility that emission is taking place without formation of a Taylor cone. This intriguing possibility needs to be confirmed through further experimentation.

Acknowledgments

The thruster was fabricated using the MIT Microsystems Technology Laboratories (MTL) facilities. We thank the MTL staff for their invaluable support. Funding for this work was provided by the Air Force Office of Scientific Research, Mitat Birkan monitor, the Space and Naval Warfare Systems Center award N66001-04-1-8925, manager Richard Nguyen, and the US Army Soldiers Systems Command award W911QY-05-1-0002, manager Henry Girolamo.

References

[1]Gassend, B., Velásquez-García, L. F., Akinwande, A. I., and Martínez-Sánchez, M., "A Fully Integrated Microfabircated Externally Wetted Electrospray Thruster," *Proceedings of the 43nd AIAA/ASME/SAE/ASEE Joint Propulsion Conference and Exhibit*, July 2007.

[2]Taylor, G. I., "Disintegration of Water Drops in an Electric Field," *Proceedings of the Royal Society of London*, Vol. 280, No. 1382, July 1964, pp. 383–397.

[3]Lozano, P. C., "Energy properties of an EMI-Im ionic liquid ion source," *Journal of Physics D: Applied Physics*, Vol. 39, 2006, pp. 126–134.

[4]Paine, M. D. and Gabriel, S., "A Micro-Fabricated Colloidal Thruster Array," *Proc. 37th AIAA/ASME/SAE/ASEE Joint Propulsion Conference and Exhibit*, AIAA, Washington, DC, July 2001, 2001-3329.

[5]Velásquez-García, L. F., Akinwande, A. I., and Martínez-Sánchez, M., "A Micro-fabricated Linear Array of Electrospray Emitters for Thruster Applications," *Journal of MicroElectroMechanical Systems*, Vol. 15, No. 5, Oct. 2006, pp. 1260–1271.

[6]Velásquez-García, L. F., Akinwande, A. I., and Martínez-Sánchez, M., "A Planar Array of Micro-Fabricated Electrospray Emitters for Thruster Applications," *Journal of MicroElectroMechanical Systems*, Vol. 15, No. 5, Oct. 2006, pp. 1272–1280.

[7]Cardiff, E. H., Jamieson, B. G., Norgaard, P. C., and Chepko, A. B., "The NASA GSFC MEMS Colloidal Thruster," *Proceedings of the 40th AIAA/ASME/SAE/ASEE Joint Propulsion Conference and Exhibit*, July 2004.

[8]Xiong, J., Zhou, Z., Sun, D., and Ye, X., "Development of a MEMS based colloid thruster with sandwich structure," *Sensors and Actuators A*, Vol. 117, 2005, pp. 168–172.

[9]Alexander, M. S., Stark, J., and Smith, K. L., "Electrospray Performance of Microfabricated Colloid Thruster arrays," *Journal of Power and Propulsion*, Vol. 22, No. 3, May–June 2006, pp. 620–627.

[10]Gassend, B., Velásquez-García, L. F., Lozano, P., Akinwande, A. I., and Martínez-Sánchez, M., "A Microfabircated Electrospray Thruster using Ridge Emitters and Ceramic-Ball Extractor Location," *Proceedings of the 42^{nd} AIAA/ASME/SAE/ASEE Joint Propulsion Conference and Exhibit*, July 2006.

[11]Velásquez-García, L. F., Akinwande, A. I., and Martínez-Sánchez, M., "Precision Hand Assembly of MEMS subsystems using meso-scaled DRIE-patterned deflection Spring Structures: An Assembly Example of an Out-of-plane Substrate Assembly," June 2007.

[12]Gassend, B., Velásquez-García, L. F., Akinwande, A. I., and Martínez-Sánchez, M., "Mechanical Assembly of Electrospray Thruster Grid," *Proceedings of the 29^{th} International Electric Propulsion Conference*, Nov. 2005, IEPC 2005-101.

[13]Gassend, B., *A Fully Microfabricated Two-Dimensional Electrospray Array with Applications to Space Propulsion*, Ph.D. thesis, Massachusetts Institute of Technology, May 2007.

[14]Fuller, J., Carlin, R. T., and Osteryoung, R. A., "The Room Temperature Ionic Liquid 1-Ethyl-3-methylimidazolium Tetrafluoroborate: Electrochemical Couples and Physical Properties," *Journal of the Electrochemical Society*, Vol. 144, No. 11, Nov. 1997, pp. 3881–3886.

[15]Jenkins, R., Gould, R. W., and Gedcke, D., *Quantitative X-Ray Spectrometry*, Marcel Dekker, Inc., 1995.

[16]Iribarne, J. V. and Thompson, B. A., "On the evaporation of small ions from charged droplets," *Journal of Chemical Physics*, Vol. 64, No. 6, 1976, pp. 2287–2294.

[17]Lozano, P., *Studies on the Ion-Droplet Mixed Regime in Colloid Thrusters*, Ph.D. thesis, Massachusetts Institute of Technology, Feb. 2003.

[18]Prewett, P. D. and Mair, G. L. R., *Focused ion beams from liquid metal ion sources*, Research Studies Press, 1991.